JOURNAL OF GUIDANCE, CONTROL, AND DYNAMICS
Vol. 17, No. 1, January–February 1994

Approach Navigation for Delivery of Small Landers to the Surface of Mars

M. Hechler* and M. Lauer†
European Space Operations Centre, 64293 Darmstadt, Germany

This paper presents the navigation analysis executed as part of the MARSNET phase A feasibility study. In the current mission baseline of MARSNET, several entry vehicles are assumed to be delivered to Mars by a common cruise spacecraft (multiprobe scenario). The achievable landing accuracy as a function of the different tracking types, and of the probe targeting and separation strategies, has been studied. In multiprobe and single probe mission scenarios landing accuracies of less than 100 km can be achieved using quasar-relative differential very long baseline interferometry (ΔVLBI) ground tracking. By means of differential VLBI tracking of the approaching spacecraft relative to a spacecraft in orbit around Mars, this delivery error can be reduced to less than 30 km.

Introduction

MARSNET is one of the four missions for which phase A studies are currently being performed in preparation for the next selection of a medium-size project (M2) in the European Space Agency (ESA) scientific program. The objective of the MARSNET mission is to execute scientific observations on three or four small stations on the surface of Mars. The operations of these stations should last for at least one Martian year.

The project was envisaged in cooperation with NASA: the ESA landers are assumed to be part of a global network of up to 16 stations distributed over the surface of Mars. At the start of phase A the mission scenario was the one developed in an assessment study in 1990: 1) The ESA landers are carried to Mars on a cruise spacecraft provided by NASA. 2) At various intervals before arrival at Mars (10 days to a few hours) the entry vehicles containing the landers separate from the cruise spacecraft. 3) From then on they are passive (spin-stabilized, unguided entry) and without communication until landing. 4) The landers utilize a NASA-operated relay satellite at Mars for communications.

The cruise spacecraft executes orbit maneuvers such that the entry probes are delivered one after the other to ballistic trajectories which reach the desired entry points and finally the landing points. Rather low entry angles (from -15 to -30 deg) are targeted, to ensure parachute opening (e.g., at Mach 1.2) at a sufficient altitude above the surface.

A question to be answered was whether a requirement on the landing accuracy, imposed by scientific or safety reasons, may influence the major decision in mission design: either to deliver several landers by one cruiser or to fly separate vehicles from Earth. The landing error largely depends on the accuracy at which the vehicles are delivered to entry, which in turn depends on the accuracies of the orbit determination and the maneuver execution, the probe separation error, and in particular, on the flight time after the last orbit correction.

The reachable landing accuracy will thus be related to the navigational means, such as the available measurement types, the calibration capabilities of maneuvers, and the accuracy of the attitude control. Also the capabilities of the ground operations system; the delays between data acquisition and maneuver executions; the operations scheduling of probe separations; and the retargeting, tracking, and orbit corrections are all issues to be discussed as part of the navigation analysis.

A thorough analysis of the orbit determination during Mars approach is given in Ref. 1. A detailed account is given there of the advanced performance properties of the NASA deep space network (DSN) of ground stations, expected in the year 2000 time frame. A new DSN capability of spacecraft to spacecraft differential very long baseline interferometric (VLBI) tracking with the two spacecraft not in the same antenna beam is presented in Ref. 2, and an analysis of its application to the MESUR Mars approach can be found in Ref. 3.

The navigation analysis presented in this paper generally follows the lines of Ref. 1, with an emphasis on the peculiarities of MARSNET, such as the effects of targeting maneuvers and the separations of several spacecraft as well as the mapping through a ballistic entry. Deterministic targeting and probe separation maneuvers and statistical orbit correction maneuvers with their execution errors are handled by a linear guidance algorithm combined with a sequential square root information filter. Only the stochastic aspects of navigation and targeting during the cruise and the approach to Mars are presented. The deterministic process of targeting to different landing points on Mars is the subject of Ref. 4.

Methods and Assumptions

Navigation Covariance Analysis Algorithm

Covariance analysis for orbit determination deals with the statistical properties of the deviation of the estimated state $\hat{x}$ from the real state x. Statistical maneuver analysis deals with the deviation of the real state x from some desired or reference state $\bar{x}$ or, more precisely formulated, with the deviation of the predicted real state from some final reference conditions. The statistical properties, e.g., the propellant estimates, thus depend on statistics of $\hat{x} - x$ and $x - \bar{x}$. Linearizing with respect to a reference trajectory, starting with initially Gaussian distributed random variables, and assuming bias free estimators and process noises, which are Gaussian, leads to the usual Kalman-type algorithms of covariance propagation and updates in the state estimation and to corresponding algorithms of linear guidance for the maneuver statistics.[5] The distributions of the random variables involved will remain Gaussian.

The covariance matrices C and P of the state deviations $x - \bar{x}$ and $\hat{x} - x$ are called dispersion and knowledge, respectively. The navigation covariance algorithm deals with the

Received July 31, 1992; presented as Paper 92-4587 at the AIAA/AAS Astrodynamics Conference, Hilton Head, SC, Aug. 10–12, 1992; revision received March 5, 1993; accepted for publication April 13, 1993.

*Mission Analyst, Mission Analysis Section, Mission Operations Department.

†Visiting Scientist, Mission Analysis Section, Mission Operations Department.

time evolution of these two matrices that undergo three transformations: 1) time propagation, 2) measurement updates, and 3) maneuver updates. Both matrices are propagated in parallel by means of the same algorithm. Measurements do not affect C, but do improve the knowledge P. Maneuvers change C (orbit corrections reduce the dispersion), but they also affect P by addition of the mechanization error. The state vector (state of the spacecraft, Mars, and possibly an observed object) is extended by colored noise parameters and bias parameters.

The bias parameters can either be handled as estimated state variables or they can be "considered." This means their subpart of the knowledge is kept at the initial value. All bias parameters in the problem under investigation are related to measurements. The state deviation (dispersion C) is not related to measurements, and so the biases do not appear in C initially. The bias parameters are introduced into the real state deviation through correction maneuvers, regardless of whether they are estimated or considered. Corresponding to actual practice, the formal estimate of the reduced state ignoring biases may be used in the maneuver calculation. Also, the estimates of the colored noise parameters (they are always part of the estimated state) may be used in the maneuver calculation. The navigation algorithm has been implemented in a sequential square root information array form with up to 42 state variables.

Orbit Calculation

The reference trajectory, along which all partial derivatives (required for the linearized statistics) are calculated, is generated by seminumerical integration from perigee to landing on the surface of Mars. The exact trajectory is obtained starting from the patched conics launch window information using a recursive quadratic programming method to match the trajectory conditions at two points, with integrations forward from Earth pericenter and backward from Mars atmospheric entry. The core of the orbit calculations is a multiconic method, according to Stumpff and Weiss,[6] which is particularly well suited to integrating simultaneously the orbits of several bodies through the transition zones at the spheres of influence. State transition matrices, and thus the gradients used in orbit matching, are generated without numerical differentiation based on the method of Goodyear[7] for the single conics. The step size of the integrator is controlled by a type of regularization that limits the integration error to that generated by a given bounding acceleration.[5]

The integration from entry into the Mars atmosphere to the surface is done by numerical single step integration with numerical differentiation. This is used to generate the mapping matrix from entry state (at fixed time) to surface coordinates (variable time and altitude). It includes a sequence of parachute openings. The atmospheric model is based on Mars global reference atmosphere model (MARSGRAM) for the actual time and location.

In the case of optical navigation or spacecraft-spacecraft interferometry, a third body, either Phobos or the orbiter, is included in the integration. The Earth is always included as a perturbing body. The effects of other planets, radiation pressure, and J_2 of the Earth have not been included for this navigation study. Important terms in the state transition matrix in the integration of several bodies are the derivatives of the states of the spacecraft and the Mars relay orbiter or the Martian moon, Phobos, with respect to the initial state of Mars.

Reference Trajectory

The reference transfer to Mars has been chosen somewhere in the middle of the 2001 window for a DELTA 7925 launch vehicle (1000-kg launch mass) with a launch date of Feb. 26, 2001, and an arrival date of Nov. 22, 2001.

The coordinates of the four reference landing points on the surface of Mars, which have been selected for the case of delivery of several landers by the cruise spacecraft, are given explicitly in Table 5. If only three landers are to be delivered at a time, then the first landing point, the antipode, will be deleted from the sequence and the interplanetary cruise will be targeted to the second point, the reference landing site.

Ground Tracking

The details of modeling the ground tracking measurements of range and Doppler as well as the different types of very long baseline interferometry (VLBI), using range and Doppler simultaneously from different ground stations and possibly also to different spacecraft, are quite complicated. In particular, the high precision tracking of a deep space probe requires modeling of a variety of perturbing effects, e.g., relativistic effect on the light time, or tropospheric and ionospheric effects. To obtain basic information on the precision that can be obtained, complex models need not be employed. Essentially, the error that remains after modeling enters the navigation analysis; the simplest model that correctly represents the geometry then usually will be adequate. In the current study, range and Doppler are simply taken as Euclidean one-way range (ground station to spacecraft) and its time derivative. All VLBI types are derived from these.

The performance assumptions, expected to be valid for the year 2001, have been taken mainly from Ref. 1. The ranging accuracy (σ = 2-m random error, 2-m bias) assumes dual frequency calibration of the electron content along the signal path. The Doppler accuracy is taken to be 0.1 mm/s. Two-way range and Doppler data are assumed to be obtained from one station at a time. The station with maximum elevation to the spacecraft is selected in overlap times. The sampling interval for range related measurements has been taken to be 30 min; for Doppler it has been taken to be 10 min, although Doppler data could be taken more frequently. In most of the simulations lower sampling rates have been taken.

VLBI data are created by simultaneously viewing a radio source by two widely separated tracking stations. The signals are brought together and correlated to obtain precise differential range (wideband VLBI) or differential range rate (narrowband VLBI). ΔVLBI measurements are formed by differencing the VLBI data of the spacecraft and an angularly nearby quasar or another spacecraft, e.g., an orbiter at Mars, resulting in delta differential one-way range (ΔDOR) or delta differential one-way Doppler (ΔDOD). In this manner the angular position and velocity of the spacecraft relative to the radio frame formed by the catalog of well-known quasars, or even the Mars reference frame in case of differencing with an orbiter, can be determined. The accuracy of these measurements (ΔDOR: σ = 30 cm, bias = 20 cm, ΔDOD: σ = 0.04 mm/s, bias = 0.04 mm/s) is much higher than that of conventional tracking data because of cancellation of common transmission media and station location errors during the differencing process. For ΔDOR one-way signals are utilized, requiring some special equipment on the spacecraft to generate the range signal.

Two variants of spacecraft-spacecraft VLBI have been studied. The first is same beam interferometry (SBI) where the angular separation of the two spacecraft is so small that they simultaneously lie within the beamwidths of the Earth-based antennas. The random errors assumed for this measurement type are 1 mm for delta differential ranging in S band (0.26-deg beam width) and 0.2 mm for X band (0.075-deg beam width). The corresponding biases are assumed to be 1 mm and 0.1 mm, respectively.

For the second type of spacecraft-spacecraft VLBI presented in Ref. 3, the two spacecraft need not be seen in the same antenna beam. We call it spacecraft-orbiter differential one-way range (SODOR).

Upgrades of the DSN VLBI system are scheduled to provide this SODOR capability in 1995 (multichannel closed-loop digital tracking receiver). Both spacecraft are to transmit the same ranging tones spread $\pm$ 20 MHz around the 8.4 GHz

X-band carrier. The two ground stations visible from the spacecraft during the VLBI tracking pass (the baseline) simultaneously track the ranging tones; first 60 s from the one spacecraft are tracked, then they sweep (60-s duration) to the other spacecraft, track this for 120 s, and sweep back to the first spacecraft for another 60 s ranging. The initial observable is the group delay of the signal arrival time at the two stations. The final observable is formed by interpolating the initial observables from each spacecraft, relating them to the same epoch, and finally taking differences between the spacecraft. For angular separations of less than 4 deg, a random error of $\sigma = 5$ cm and a bias of 2 cm are assumed for SODOR. For higher angular separations the tracking type remains useful with some deterioration, but this is not relevant for the Mars approach. Station coordinate biases of 10 cm have been assumed.

Optical Measurements

As an option, optical navigation is assumed to be done by tracking an object, in the current case the Martian moon, Phobos, against the background of fixed stars. At large distances Phobos will appear on the images like a star. At closer approach it may extend over several pixels. When imaging Phobos and the fixed stars in the same frame any camera pointing error will cancel. This means a high precision direction observation from the spacecraft to Phobos is obtained.

Phobos is dynamically tied to Mars, so knowledge of Mars' ephemeris will improve by tracking Phobos. The use of different cameras characterized by different fields of view and pixel sizes has been analyzed.[8]

Launcher Injection Error

The initial dispersion at injection into an escape orbit depends to a large extent on the guidance system of the upper stage of the launch vehicle used for the injection.

For the Delta 7925 the altitude error in the parking orbit and the error in the velocity increment to be provided by the upper stage have been derived from information for low orbits and geostationary transfer orbit contained in Ref. 9. The parking orbit altitude error has been taken to be 18.5 km (3σ). The upper stage velocity increment is $\Delta v_p = 3.64$ km/s. The 3σ error in the size of this Δv is taken to be 0.5%.

Midcourse Maneuvers

We distinguish two types of maneuvers: 1) deterministic maneuvers and 2) correction maneuvers.

Deterministic maneuvers are part of the reference orbit. They do not depend on any stochastic information. Typical deterministic maneuvers are the targeting maneuvers at Mars approach. The effect of a deterministic maneuver that enters the navigation analysis is the maneuver execution error. To model this, an error in the size of the maneuver, in the form of a percentage, and an error in the direction, in the form of a cone angle around the reference direction, are assumed. Assuming a uniformly distributed phase angle on the error cone allows the transformation of the two quantities to an error covariance matrix for the three-dimensional Δv vector.

Statistical orbit correction maneuvers are calculated to correct the orbit such that a target state is reached. In this calculation the estimated state deviation

$$\tilde{x} - \hat{x} = (x - \hat{x}) - (x - \tilde{x})$$

is used. The target state is defined by the deviation of the position at a fixed final time. In the guidance the propagation through the Mars atmosphere is not used. The trajectory integration stops at pericenter of Mars, ignoring the atmosphere. The mapping to the landing point is then done by propagating back to the entry point on an unperturbed hyperbola and then forward to the landing with the full rotating frame entry dynamics.

Table 1 Process noise assumptions

	σ_0	σ_p	τ_p
Radiation pressure	0.1	0.1	100 days
Spacecraft coordinate accelerations	10^{-7} km/s^2	10^{-7} km/s^2	7 days
Orbiter coordinate accelerations	10^{-9} km/s^2	10^{-9} km/s^2	0.1 days

The guidance algorithm described in Ref. 5 has been extended to include the Mars state as well as the components of the extended state vector that describe the colored noise and the consider biases. The propellant estimates for the correction maneuvers are obtained from the statistics of the estimate of $|\Delta v|$. The results are expressed by percentiles since $|\Delta v|$ does not have a Gaussian distribution.

The maneuver execution error for statistical orbit corrections will depend on the statistics of the parameters describing the maneuver itself, so it will be randomized as well. With the same linearizations as for the deterministic maneuvers the mechanization error can be stated as a function of the maneuver error and of the covariance estimate of the stochastic maneuver. The reference error assumptions taken for size and cone angle of deterministic and stochastic maneuvers are

$$3\sigma_{\Delta v} = 1.5\% \times \Delta v, \qquad 3\sigma_\theta = 1 \text{ deg}$$

These error assumptions will require a high-quality attitude control and good thruster calibration.

Entry Vehicle Separations

In the navigation algorithm separations are handled like deterministic maneuvers. This means errors are defined in terms of percentage and cone angle relative to the separation Δv.

The inertial Δv acting on the separated body is calculated as a function of the two separating masses and a given total relative velocity, or for a given energy stored in the separation springs. The separation attitude is chosen as required at the later entry, in the direction of the velocity relative to the rotating atmosphere at entry.

The current baseline is to size the springs such that very small separation velocities (10 cm/s) are generated. This results in small errors introduced by the separations. The orbit targeting and attitude acquisition is assumed to be done by the cruise spacecraft before the separations, and the time sequence has been chosen to allow for tracking between targeting and separation as well as for additional statistical orbit correction maneuvers to remove the errors introduced by the targeting maneuvers.

Process Noise

The dynamic equations are extended by introducing colored noise parameters into the state vector. The parameters are assumed to be chosen such that their dynamics matrix has diagonal terms

$$m_p = -(1/\tau_p)$$

The correlation times τ_p, the steady-state standard deviations of the continuous processes σ_p, and the initial variances σ_0 are assumed as given in Table 1. The acceleration noises are set artificially high to stabilize the filter.

Ephemeris

The planet ephemerides are taken from the Jet Propulsion Laboratory ephemeris file DE118. To calculate the uncertainty in the position of Mars at the time of arrival of the spacecraft, a covariance matrix derived from a diagonal Brouwer Clemence set III element covariance matrix with the standard deviations from Ref. 10 is propagated, assuming only heliocentric Keplerian motion of Mars to simplify the

Table 2 Midcourse corrections propellant

	Time, day	Mean, m/s	σ, m/s	99%, m/s	99.7%, m/s
First correction	10	43.9	22.4	107.9	122.5
Midcourse	50	0.34	0.19	0.92	1.05
Midcourse	180	0.03	0.02	0.10	0.12
Approach	249	(see Mars Approach Navigation section)			

Table 3 Single probe delivery error (3σ km)

Tracking types	Time of data cutoff		
	Day −5	Day −1	Day −0.1
Doppler only	244	205	103
Range and Doppler	329	318	158
Quasar-ΔDOR only	112	101	100
Quasar-ΔDOD only	170	100	95
ΔDOR, range, Doppler (reference)	110	88	75
SODOR (X band), range, and Doppler	30	9	—
SBI (S band), range, and Doppler	—	24	3
Optical (6 μrad), range, Doppler	75	19	—

computation of transition matrices. Alternatively, the initial state covariance matrix for Mars has been calculated by running the navigation software with the reference tracking assumptions (ground VLBI) for a relay satellite orbiting Mars.

The Martian satellite Phobos moving in a nearly circular orbit at an altitude of about 6000 km may be used for optical navigation as explained earlier. A high orbital accuracy is not needed for the purpose of navigational considerations, and therefore an orbit model simplified from Ref. 11 has been employed.

Cruise Navigation

Propellant Allocation

Orbit determination during the cruise phase (from launch to Mars approach at day −20 from arrival) can be based on conventional deep space tracking. Range and Doppler tracking is assumed at a typical rate of 20 points per day in the first 10 days after Earth departure and during periods of about one week before midcourse corrections. Assumptions on the tracking accuracy are not essential.

Midcourse correction maneuvers will have to be scheduled to remove the injection error of the perigee burn of the launch vehicle upper stage and to compensate for other stochastic perturbations that act on the spacecraft but which had not been foreseen in the planning of the trajectory when the perigee injection maneuver was optimized. Fixed time of arrival guidance is assumed (the landing sites are fixed). Some statistics for a typical sequence of orbit correction maneuvers are given in Table 2.

The times are counted from injection into interplanetary transfer at perigee. The given percentiles are calculated using the statistical properties of the estimate of $|\Delta v|$. The scheduling of the cruise maneuvers, taken to be at day 50 and day 180, is not critical.

The size of the first orbit correction maneuver will depend on its execution time, being slightly reduced if it can be executed earlier. The essential dependence will be on the launcher error. The perigee injection error, mainly in the size of the velocity increment, is the dominating source of the trajectory error that has to be corrected, but the altitude error in the parking orbit also has a considerable effect.

Mars Avoidance

Before targeting to entry conditions, a fly-by point at Mars will be chosen at a high enough altitude to ensure that the upper stage of the launch vehicle, and also the spacecraft in failure cases, do not impact Mars. For the Delta 7925, the projection of the 1σ launch vehicle dispersion into the B plane at Mars (orthogonal to hyperbola asymptote) for the reference case has the axes

$$a = 2.47 \times 10^6 \text{ km}, \qquad b = 0.11 \times 10^6 \text{ km}$$

In the B plane the impact disk of Mars will have a radius of $\Delta = 5448$ km. Assuming a Gaussian distribution, one can easily conclude that when targeting with a Delta upper stage to the center of Mars, the probability of hitting Mars is

$$P_{\text{hit}} < 5.48 \times 10^{-5}$$

If this is not low enough, one may choose the target point outside the impact disk. Assuming the $n\sigma$ ellipse just touches the impact disk and limiting the probability P_{hit} to hit Mars renders n as a function of P_{hit}.

Targeting the launcher to such a "miss point" introduces a penalty on the first orbit correction maneuver to retarget to the actual desired entry conditions, in combination with the removal of the launch vehicle error. The center points $x_M(\tau)$ of all $n\sigma$ ellipses that touch the impact disk lie on an ellipse around zero. For each initial target point $x_M(\tau)$ on this ellipse, a random sample of impact points x in the B plane can be generated. Maneuver statistics of $|\Delta v|$ at day 10, to move the random impact points x to the actual entry target point x_T for the optimum choice of τ have been accumulated using a random sample of 10^5 state vector deviations.

For a 1σ off targeting, the impact probability P_{hit} is less than 3.3×10^{-5} at virtually no penalty in $\Delta v - \Delta v_0$. For a 2σ and 3σ off targeting, impact probabilities of $P_{\text{hit}} < 7.4 \times 10^{-6}$ and $P_{\text{hit}} < 1.0 \times 10^{-6}$ are reached at propellant penalties of 8 m/s and 21 m/s, respectively. The stated propellant penalty $\Delta v - \Delta v_0$ is the difference of the 99 percentile with $n\sigma$ off targeting and the 99 percentile with targeting to x_T directly at launch (which is 100 m/s).

Mars Approach Navigation

The initial dispersion and knowledge covariances of the spacecraft state in inertial space (six dimensional) are generated by using the navigation algorithm from launch to day −10 from arrival and multiplying the resulting covariance matrices by 10. The correlations to the noise parameters and the bias parameters are set back to zero, and the variances of these parameters are reinitialized. Statistical orbit corrections are scheduled at days −8, −5, and −1 from pericenter passage (arrival) at Mars.

Parametric Study for Single Probe Scenario

For the single probe scenario an extensive sensitivity analysis has been performed by varying all assumptions by an order of magnitude, one by one.[8] The mapped landing knowledge is not unexpectedly sensitive to the initial covariance, the process noise models, the tracking accuracies, the initial ephemeris errors, and the filtering technique.

Table 3 shows the reachable landing accuracy for a single probe delivered to the reference landing point (entry angle −17 deg) for some of the combinations of tracking types. The given landing error value is the (full) major axis of the 3σ error ellipse in kilometers. The error ellipse is obtained from the eigenvalues of the 2×2 covariance matrix at the surface intersection. The knowledge covariance is mapped from three times of data cutoff that appear typical for different approach scenarios. It can be assumed that a last orbit correction maneuver is done with some delay after this data cutoff time, corresponding to the time required for communications and ground processing. The passive entry probe is separated imme-

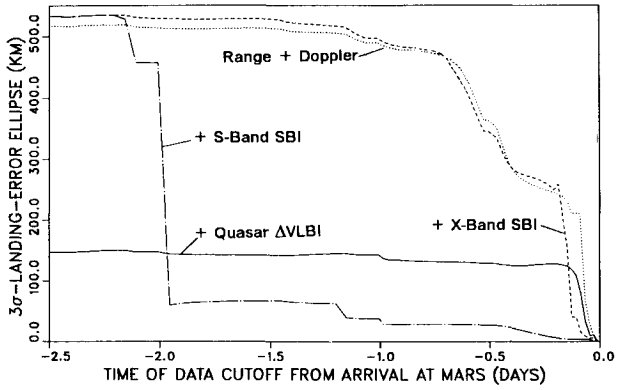

Fig. 1 Single probe landing error: quasar ΔVLBI.

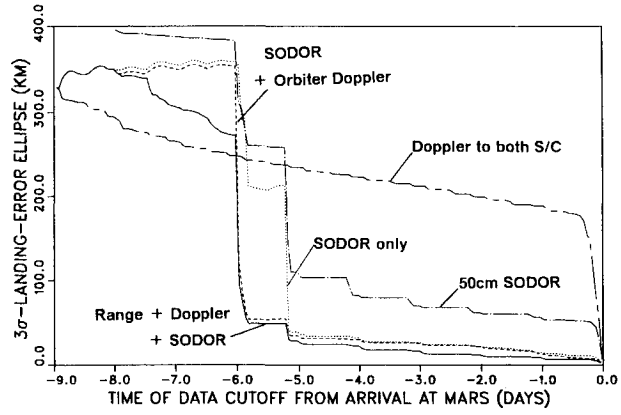

Fig. 2 Single probe landing error: spacecraft orbiter ΔVLBI.

diately after this last correction maneuver. In all cases the considered-covariance algorithm has been used, which explains the unnatural effect, for example, that Doppler alone appears better than range and Doppler. The bias covariances have been chosen to be unduly conservative. This has been done because some error sources that may affect ranging, e.g., the Earth ephemeris errors, have been neglected, with the intention to reduce the weight of ranging with respect to those tracking types that are less sensitive to modeling errors.

Figure 1 compares the cases except SODOR. In the single probe scenario the execution errors of the statistical orbit corrections do not play a role; they are not visible in the figure. The dotted line shows the major axis of the 3σ delivery error ellipse on the surface of Mars, mapped from different times of cutoff of range and Doppler tracking data. The improvement of the delivery error observed for very late data cutoff time (-0.1 days) is due to the dynamic effect of the Mars gravity field acting on the approaching spacecraft, which can be observed in the Doppler data. The continuous line shows the mapped delivery error when quasar-ΔVLBI tracking is done in addition to range and Doppler; the dash-dot line gives the mapped error if same beam interferometry (SBI) in the S band replaces the quasar ΔVLBI; and finally the dashed line shows the corresponding mapping with X-band SBI. Rather low tracking frequencies have been used (about every 30 min). If a smaller time interval for tracking is used, the results are not much affected. The essential contribution to the targeting accuracy comes from the differential VLBI tracking types, but range and Doppler still contribute.

In particular, this is the case for the spacecraft-orbiter ΔVLBI tracking (SODOR) by the assumed simultaneous orbiter ranging. Figure 2 shows the outstanding performance of the SODOR tracking type, even in a deteriorated form. The

Table 4 Reference case error mapping

	Surface		Entry point		*B* plane	
Day	a, km	b, km	γ_e, deg	h_e, km	a, km	b, km
−5	108	6	0.28	10.9	33.6	6.3
−1	86	3.5	0.18	8.6	26.8	3.8
−0.5	77	3.2	0.17	7.8	24.0	3.5
−0.1	72	1.4	0.12	4.9	21.5	2.0
−0.02	28	1.4	0.04	1.0	9.9	0.9

continuous line shows the mapped delivery error for SODOR with simultaneous spacecraft and orbiter ranging and Doppler tracking. The dotted and dashed lines show the corresponding errors without orbiter tracking and with orbiter Doppler tracking only, together with the SODOR. The dash-dot line assumes a deteriorated SODOR accuracy (50 cm) together with Doppler to both spacecraft. The other line (long dash-short dash) compares with Doppler only, no SODOR. To display clearly the effect of the different tracking types, the orbiter tracking is turned on at day -8 from arrival at Mars. The SODOR is turned on at day -6 although both tracking types could be used much earlier and would then lead to much better delivery accuracies at an earlier data cutoff. Except for optical navigation, which requires complex spacecraft and ground systems and operations, SODOR appears to be the only tracking type that ties the approaching spacecraft to the Mars reference frame, removes the effect of the Mars ephemeris error, and allows early enough orbit correction maneuvers for precise targeting.

With SODOR, targeting accuracies below 30 km (3σ) can be reached several days before arrival (without the errors introduced during the atmospheric flight). Ranging of the orbiter further improves the targeting. The independence from angular separation of the two tracked spacecraft for this X-band differential tracking type provides a large flexibility in arrival scheduling. High accuracy can be reached early, and probe operations can be scheduled in sequence in the single probe scenario.

The dashed and dotted lines in Fig. 2 show that the tracking type is also very powerful without orbiter ranging or even without any simultaneous tracking of the orbiter. The orbit of the relay spacecraft in that case will not be known to the 20-m level as in the case with range and Doppler; the achieved accuracy of several 100 m is still sufficient to relate the approaching spacecraft to the Mars frame. The dash-dot line shows the corresponding results for a strongly deteriorated VLBI system, the dash-dash line gives a comparison without any VLBI.

Mapping to Entry Point and *B* Plane

Table 4 gives a comparison of the delivery error for the reference case (quasar-ΔVLBI) mapped to different final points. The covariances are propagated numerically from the time of data cutoff to the pericenter passage at Mars (without atmosphere) as in the previous analysis. Then the linear transformation is generated from pericenter state deviation to entry altitude and entry angle deviation at the time of entry, or to the B-plane coordinates, assuming Keplerian motion. With the thus generated 6×2 transformation matrix the entry parameter and B-plane variances can be calculated from the pericenter state covariance matrix. The orientation of the target plane ellipses is not given in the table. On the surface it is about -28 deg from east. The axes a and b of the error ellipses are calculated by eigenvalue transformation. All stated numbers are 3σ errors. The times in the first column are times of data cutoff as in the previous tables; a maneuver execution delay is not taken into account.

Multiprobe Approach Navigation

For targeting several probes to different landing points using the attitude and orbit control system of a sophisticated

Table 5 Mapped landing error ellipses for multiprobe scenario

Maneuver	Δv, m/s	Time, days	Landing point		3σ landing error		
			λ, deg	θ, deg	a, km	b, km	ω, deg
Separate to antipode (site 1)	0.09	−10.2	100.51 E	12.91 N	a) 50.0	17.0	59.0
					b) 6.9	2.1	54.7
Retarget to reference (site 2)	11.20	−10.0	45.96 W	15.60 N	a) 1125	100.3	−36.5
					b) 558.2	79.5	−36.6
Correct 99%	0.17	−8.0					
Correct 99%	0.15	−4.4					
Separate to reference	0.09	−4.2			a) 191.6	6.6	−28.4
					b) 13.3	0.5	−29.2
Retarget to site 3	18.70	−4.0	128.46 E	27.54 S	a) 237.5	131.8	−87.0
					b) 116.0	64.5	−85.0
Correct 99%	0.50	−2.4					
Separate to site 3	0.08	−2.2			a) 77.9	8.2	78.0
					b) 6.8	0.9	77.0
Retarget to site 4	13.60	−2.0	77.00 E	37.33 S	a) 305.5	65.0	−31.4
					b) 149.2	21.1	−29.6
Correct 99%	0.35	−1.2/−0.8					
Separate to site 4	0.08	−0.6			a) 78.3	21.8	−66.9
					b) 4.1	1.7	−68.4

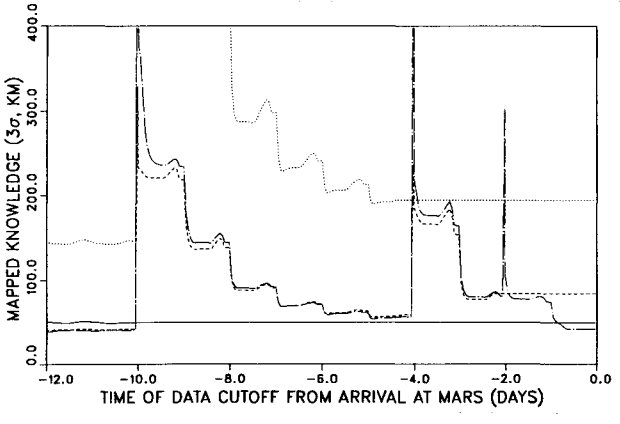

Fig. 3 Mapping of knowledge with multiprobe targeting sequence: quasar ΔVLBI.

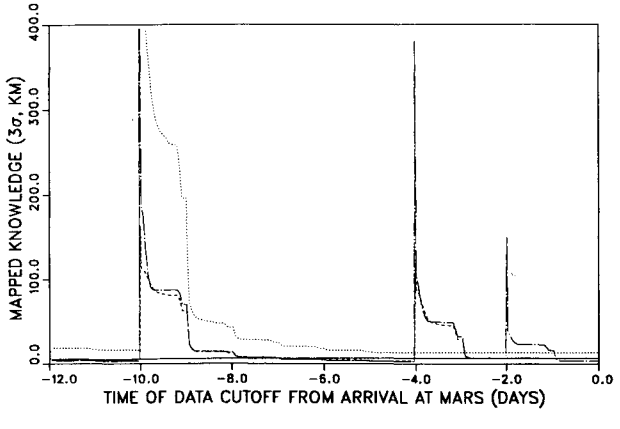

Fig. 4 Mapping of knowledge with multiprobe targeting sequence: spacecraft orbiter ΔVLBI.

cruise spacecraft, only one reference scenario has been studied so far. The assumptions made on the desired landing sites have not taken into account any feedback from this navigation analysis. Also they are not representative for the scientific requirements. Table 5 compares two cases for the prime options of tracking systems: 1) quasar ΔDOR and 2) spacecraft-spacecraft ΔDOR (SODOR).

The size and orientation of the 3σ landing error ellipses at the four reference landing locations are given. The error ellipses are mapped from immediately after the retargeting maneuvers and after the orbit correction maneuvers that are scheduled to allow accumulation of sufficient tracking data between the separations. The maneuver execution delay is taken to be 5 h for quasar ΔVLBI. The process noise in this case has been reduced to 10^{-9} km/s^2 steady-state variance, because of the long mapping intervals from separations to landing, without tracking. For quasar-ΔVLBI tracking, except for the reference landing site (entry angle = − 17 deg) delivery errors below 100 km (3σ) can be reached in all cases. For the reference site, even in the case of very precise maneuver execution, the delivery error remains above 160 km. To reduce this error the targeting sequence could be modified.

Figure 3 shows the mapped knowledge as a function of data cutoff time for each of the landers for case a of Table 5: the continuous line for the antipode, the dotted line for landing site 2 (reference), the dashed line for site 3, and the dash-dot line for site 4. It can be observed that the mapped delivery errors remain constant from the times of probe separation because the separated probe is neither tracked nor maneuvered. The peaks are introduced by the execution errors of the retargeting maneuvers. The state dispersion is not shown; it increases accordingly at the retargeting maneuvers and is then reduced to about the knowledge level, at statistical correction maneuvers that are scheduled before the separations. The different mapped knowledge levels for the same time, depending on the targeting point, are induced by the different mapping properties as a function of the atmospheric trajectories for the different entry angles. Figure 3 also displays the locations of the VLBI tracking passes (where the knowledge improves).

Clearly, even without measurements that provide state information in the Mars reference frame, an approach targeting and separation sequence as envisaged appears feasible. Possibly all probes can be delivered to an accuracy of less than 100 km from the desired point. This does not take into account the errors introduced during the atmospheric phase.[8] To reach such accuracies, restrictions on the choice of the landing points and the targeting operations must be imposed (e.g., the probe delivered first should be targeted to a steeper entry angle and thus to lower altitude landing points to ensure parachute opening).

In case b, with spacecraft-to-orbiter ΔVLBI, the only assumptions that have been changed with respect to case a are the time of the last orbit correction maneuver (it has been moved to day − 0.8 to allow more time for the completion of the last VLBI tracking pass) and the delay for ground processing and signal turnaround (it has been reduced to 1 h for the observation without quasars).

It should be noted that any error introduced during atmospheric flight has not been included. One has to foresee about another 20–30 km for shallow entry angles. Figure 4 shows the time history of the mapped knowledge error for case b.

Summary and Conclusions

A covariance analysis study has been performed for the navigation process of a reference MARSNET mission in the 2001 launch window. Software using a square root information filter and linear guidance with consider bias parameters and exponentially correlated noise processes has been used. The following conclusions can be drawn.

1) The DELTA 7925 launch vehicle introduces a considerable injection error at Earth departure which requires a propellant allocation of 100 m/s for the first midcourse correction maneuver when executed within 10 days from perigee.

2) The limit of the reachable landing accuracy on Mars using conventional range and Doppler tracking only appears to be at about 200 km. This assumes an unguided atmospheric entry at an entry angle of about − 15 deg.

3) In a single-probe scenario a delivery error of less than 100 km can be reached for the cited entry angle using additional quasar-differential very long baseline interferometry (ΔVLBI) tracking.

4) In the multiprobe scenario restrictions on the targeting sequence and the landing points relative to each other must be carefully incorporated to ensure a landing error of less than 100 km, without Mars related observables.

5) Same beam interferometry (SBI) in X band appears not to be useful, because the data type will be available only 15 h from arrival. SBI in S band will improve the delivery error to less than 50 km from about two days before arrival at Mars.

6) Optical navigation will render delivery errors better than quasar ΔVLBI, provided a narrow angle high resolution camera is utilized.

7) In both scenarios (multiprobe and single probe) the ground station beam width-independent spacecraft-to-orbiter differential one-way range in the X band (SODOR) is extremely valuable. It improves the delivery error considerably compared with quasar ΔVLBI. With orbiter ranging the landing error improves to the 10-km level (without atmospheric effects) in the single-probe scenario. Also in the multiprobe scenario the delivery errors for all landers can be below 40 km (3σ without atmospheric errors).

8) From the point of view of navigation, a preference of one of the two given scenarios cannot be stated. The decision between these two basic mission design options will be related to operations analysis and spacecraft cost analysis.

References

[1]Konopliv, A., and Wood, L. J., "High-accuracy Mars Approach Navigation with Radiometric and Optical Data," AIAA/AAS Astrodynamics Conference AIAA Paper 90-2907, Portland, OR, Aug. 1990.

[2]Edwards, C. D., Jr., Folkner, W. M., Border, J. S., and Wood, L., "Spacecraft-Spacecraft Very Long Baseline Interferometry for Planetary Approach Navigation," AAS/AIAA Spaceflight Mechanics Meeting, AAS Paper 91-181, Houston, TX, Feb. 1991.

[3]Konopliv, A., "Mars Approach Navigation for MESUR," Jet Propulsion Lab., JPL Interoffice Memo. 314.3-976, Pasadena, CA, May 1991.

[4]Lauer, M., and Hechler, M., "Targeting of Several Mars Landers," AIAA Paper 92-4588; also *Journal of Guidance, Control, and Dynamics,* Vol. 17, No. 1, 1994, pp. 109–115.

[5]Boissieres, J., and Hechler, M., "On the Midcourse Navigation for the GIOTTO Comet Halley Flyby Mission," European Space Operations Centre, MAD WP 129, Darmstadt, Germany, June 1980.

[6]Stumpff, K., *Himmelsmechanik,* Band III, DVW, Berlin, 1974, pp. 322–336

[7]Goodyear, W., "Completely General Closed-form Solution for Coordinates and Partial Derivatives of the Two-body Problem," *Astronomical Journal,* Vol. 70, No. 3, 1965, pp. 198–192.

[8]Hechler, M., and Lauer, M., "MARSNET—Phase A Mission Analysis: Navigation," European Space Operations Centre, MAS WP 324, Darmstadt, Germany, Dec. 1991.

[9]"Commercial Delta II Payload Planners Guide," McDonnell Douglas, MDC H3223B, Dec. 1989.

[10]Standish, E. M., Jr., "The Observational Basis for JPL's DE200, the Planetary Ephemerides of the Astronomical Almanac," *Astronomy and Astrophysics,* Vol. 233, No. 1, 1990, pp. 252–271.

[11]Morley, T. A., "An Improved Analytical Model for the Orbital Motion of the Martian Satellites," *Astronomy and Astrophysics,* Vol. 228, No. 2, 1990, pp. 260–274.